

# Dense granular flows: two-particle argument accounts for friction-like constitutive law with threshold

Pierre Rognon and Cyprien Gay\*

*Centre de Recherche Paul Pascal, CNRS UPR 8641 - Av. Dr. Schweitzer, Pessac, France*  
*Matière et Systèmes Complexes, Université Paris-Diderot - Paris 7, CNRS UMR 7057 - Paris, France*

(Dated: September 15, 2008)

A scalar constitutive law is obtained for dense granular flows, both in the inertial regime where the grain inertia dominates, and in the viscous regime. Considering a pair of grains rather than a single grain, the classical arguments yield a constitutive law that exhibits a flow threshold expressed as a finite effective friction at flow onset. The value of the threshold is not predicted. The resulting law seems to be compatible with existing data, provided the saturation at high velocity (collisional regime) is added empirically. The law is not exactly the same in both regimes, which seems to indicate that there is no “universal” law.

PACS numbers: 83.80.Fg 47.57.Gc 83.10.Gr 83.60.La

## I. INTRODUCTION

Dense flows of dry granular materials and granular pastes is still a surprising field of research [1]. Many complex features have already been observed, but the basic mechanisms that relate grain properties to the collective behavior are not fully identified yet. Gaining new insights into this multi-scale issue should provide robust models and rationalize a wide range of results obtained in various geometries and with various materials.

Here, we focus on the central question of the constitutive law, which relates the stresses (shear stress  $\tau$  and pressure  $P$ ) to the shear rate  $\dot{\gamma}$  in a steady and homogeneous flow. Several measurements evidenced a flow threshold with a frictional criterion: a flow stops if the ratio between the shear stress and the pressure (effective friction coefficient  $\mu = \frac{\tau}{P}$ ) is lower than a critical friction coefficient  $\mu_c$ . This is reminiscent of yield stress fluids, which stop below a critical shear stress  $\tau_c$ . But for granular materials this yield stress depends on the pressure ( $\tau_c = \mu_c P$ ). Measurements also evidenced an increase of the friction coefficient with the shear rate. Furthermore, dimensional analysis implies that the effective friction coefficient cannot depend just on the shear rate  $\dot{\gamma}$ , but rather on a dimensionless combination  $I = T\dot{\gamma}$  where  $T$  is some time scale.  $T$  is usually understood as the typical time for a single grain, accelerated by the pressure  $P$  (or force  $Pd^2$ ), to move over a distance comparable to its own size  $d$ . It has been estimated in two situations through a simple dimensional analysis. For dry grains, the surrounding fluid can be neglected and the pressure is resisted only by grain inertia (mass  $m$ ) [2]:

$$m \frac{d}{T_{\text{gi}}^2} \simeq P d^2 \quad i.e., \quad T_{\text{gi}} = \sqrt{\frac{m}{P d}}. \quad (1)$$

For granular pastes, if the grain inertia is negligible as

compared to the viscous effect of the surrounding fluid, the force  $Pd^2$  exerted by the pressure is resisted by a typical Stokes viscous drag force felt by a single grain moving at the velocity  $d/T_{\text{fv}}$  [3]:

$$\eta d \frac{d}{T_{\text{fv}}} \simeq P d^2 \quad i.e., \quad T_{\text{fv}} = \frac{\eta}{P}. \quad (2)$$

Using these time scales provided robust scaling behaviors in various flow geometries for dry grains, whether frictional or not [2, 4, 5, 6], cohesive [7, 8] or polydisperse [9], and also for immersed grains [3]. Empirical functional forms for the constitutive law were proposed to describe the measurements [2, 3, 4, 5, 6, 7, 8, 9, 10, 11, 12], for instance [3]:

$$\frac{\tau}{P} = \mu(I) = \mu_c + \frac{\mu_2 - \mu_c}{I_0/I + 1}. \quad (3)$$

This shape includes a critical friction coefficient below which flow stops,  $\mu_c$ . At large  $I$ , a saturation of the effective friction ( $\mu(I) \rightarrow \mu_2$ ) reflects the onset of the collisional regime, where grains are diluted and interact through binary collisions [2, 4, 6]. In the dense regime, at small  $I$ , the effective friction is assumed to increase linearly with  $I$  (slope  $\frac{\mu_2 - \mu_c}{I_0}$ ), and thus with the shear rate. However, a quadratic term in  $\dot{\gamma}$  was also included to fit the data in other works [10, 11, 12]. So far, there is no consensus on the shape of the constitutive law. As for the choice of a frictional form like (3), it is justified purely phenomenologically.

In this paper, we propose a simple analysis to derive such a frictional constitutive law from the grain properties. We apply this analysis first to dry grains with no fluid, then to immersed grains with no inertia, and finally to a situation with both the grain inertia and the fluid viscosity. We compare the model thus obtained to the experimental data with immersed and dry grains by Cassar *et al.* [3], kindly provided by the authors.

Hopefully, the argument presented here may later be useful to understand the origin of much complex

---

\*Electronic address: cyprien.gay@univ-paris-diderot.fr

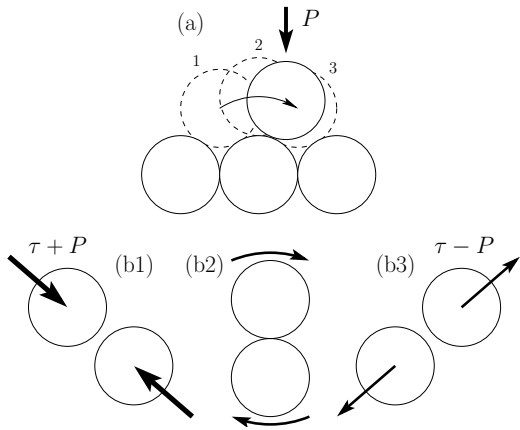


FIG. 1: Schematic evolution within the granular material during shear. (a) One grain is transported quasistatically from position 1 to position 2, then falls into position 3 due to the applied pressure  $P$ . In the present work, we rather consider a pair of grains during the period of time when they are close neighbours (b1-3). First, the deviatoric (typically, shear) component of the stress,  $\tau$ , helps the pressure  $P$  establish the contact (b1). Then, the contact rotates due to the overall material deformation (b2). Finally, the deviatoric stress overcomes the pressure to break the contact (b3). Because the pressure is compressive in a non-cohesive granular material, the typical magnitude of the force transmitted between both grains is stronger when the contact forms than when it breaks.

features of dense granular flow: the viscosity bifurcations [13, 14, 15], a critical shear rate below which no homogeneous flow exists [2, 3, 4, 14, 16] or a possible coexistence of flowing and non-flowing regions (shear-banding, shear localization, cracks) [2, 7, 17, 18, 19, 20].

## II. ONE-GRAIN VERSUS TWO-GRAIN ARGUMENT

As mentioned above, the classical approach consists in assuming that the constitutive law has a frictional form like  $\frac{\tau}{P} = \mu(I)$  and to include a characteristic time such as those provided by Eqs. (1) and (2), that reflect the motion of a single grain subjected to the pressure  $P$  in the granular material.

As shown on Fig. 1, the present approach is focused on the entire lifetime of a contact between two grains rather than on the motion of a single grain. The contact is being established when the pair of grains is oriented along a compressive direction, see drawing (b1). Hence, the deviatoric part of the stress is complemented by the pressure part to favour the approach of both grains. The opposite is true when the contact is breaking (b3): the pair is now oriented along a tensile direction, and the pressure partly resists the deviatoric part of the stress. The normal force acting on the contact is thus stronger

during the approach than during the separation:

$$F_N^{\text{app}} \simeq d^2 (P + \tau) \quad (4)$$

$$F_N^{\text{sep}} \simeq d^2 (P - \tau) \quad (5)$$

$$|F_N^{\text{app}}| > |F_N^{\text{sep}}| \quad (6)$$

where  $\tau > 0$  is the magnitude of the deviatoric stress. Note that the stress on the contact evolves as described above even if the macroscopic stress does not vary. Indeed it is the rearrangement of the neighbouring grains that induce the progressive reorientation of the pair of interest and the corresponding inversion of projection of the deviatoric stress on the pair axis.

Let us now assume that during a 100% deformation, all inter-grain contacts are typically renewed. The corresponding time  $1/\dot{\gamma}$  is then comparable with the typical lifetime of a contact:

$$\frac{1}{\dot{\gamma}} \simeq T^{\text{app}} + T^{\text{sep}} \quad (7)$$

where the value of  $T^{\text{app}}$  and  $T^{\text{sep}}$  is given by Eqs. (1) and (2), replacing the pressure by  $\tau \pm P$  as in Eqs. (4-5):

$$T_{\text{gi}}^{\text{app}} \simeq \sqrt{\frac{m}{(\tau + P)d}} \quad (8)$$

$$T_{\text{gi}}^{\text{sep}} \simeq \sqrt{\frac{m}{(\tau - P)d}} \quad (9)$$

$$T_{\text{fv}}^{\text{app}} \simeq \frac{\eta}{\tau + P} \quad (10)$$

$$T_{\text{fv}}^{\text{sep}} \simeq \frac{\eta}{\tau - P} \quad (11)$$

From Eqs. (7) and (8-9), we obtain a local scalar constitutive equation for the inertial regime:

$$\dot{\gamma} \sqrt{\frac{m}{Pd}} = \frac{1}{1 + \sqrt{\frac{\tau - P}{\tau + P}}} \sqrt{\frac{\tau}{P} - 1} \quad (12)$$

which can be approximated as:

$$\frac{\tau}{P} \simeq 1 + \dot{\gamma}^2 \frac{m}{Pd} \quad (13)$$

since the first factor in Eq. (12) varies smoothly between 1 and  $1/2$  for  $\tau > P$ .

Similarly, using Eqs. (7) and (10-11), we obtain a local scalar constitutive equation for the viscous regime:

$$\frac{\tau}{P} = \frac{P}{\tau} + \frac{\dot{\gamma} \eta}{P} \quad (14)$$

## III. DISCUSSION AND COMPARISON WITH EXPERIMENTS

When combined with Eq. (1) or (2) as appropriate, Eqs. (12) and (14) become:

$$I \simeq \frac{1}{1 + \sqrt{\frac{\tau - P}{\tau + P}}} \sqrt{\frac{\tau}{P} - 1} \quad (15)$$

$$I \simeq \frac{\tau}{P} - \frac{P}{\tau} \quad (16)$$

Even though these two equations do not reduce to Eq. (3), let us emphasize that they imply the existence of a flow threshold: flow can occur ( $\dot{\gamma} > 0$ ) only when  $\tau > P$ .

However, the *value* of the threshold, named  $\mu_c$  in Eq. (3), is not predicted in the present approach. Indeed, the qualitative argument presented earlier, that leads to a different value for the force between two particles during their approach and during their separation is not precise enough to provide any reliable prefactor for  $\tau$  in Eqs. (4-5).

As shown by Fig. 2, the saturation of function  $\mu(I)$  at large  $I$  introduced empirically in Eq. (3) is not reproduced by Eqs. (15-16), as the arguments used to obtain the adimensional parameter  $I$  for the dense flows are not compatible with the binary collisions thought to be at the origin of the saturation. However, the plots of Eqs. (15-16) are not very different from that of

$$\frac{\tau}{P} - 1 = I \quad (17)$$

(see curve  $C^\infty$  of Fig. 2), obtained from Eq. (3) with  $\mu_c = 1$ , after taking the limit  $\mu_2 \rightarrow \infty$  and  $I_0 \rightarrow \infty$  while keeping  $I_0 = \mu_2/\mu_c - 1$ , in order to remove the saturation.

Let us introduce empirically the very same saturation into Eqs. (15-16) in order to be able to test whether they are compatible with the data presented by Cassar *et al.* [3].

Eq. (3) can be rewritten as:

$$\frac{\tau/\mu_c}{P} - 1 = \frac{\mu_2/\mu_c - 1}{I_0/I + 1} \quad (18)$$

Similarly, let us transform Eqs. (15-16) into:

$$\frac{1}{1 + \sqrt{\frac{\tau/\mu_c - P}{\tau/\mu_c + P}}} \sqrt{\frac{\tau/\mu_c}{P} - 1} \simeq \frac{\mu_2/\mu_c - 1}{I_0/I + 1} \quad (19)$$

$$\frac{\tau/\mu_c}{P} - \frac{P}{\tau/\mu_c} \simeq \frac{\mu_2/\mu_c - 1}{I_0/I + 1} \quad (20)$$

Eqs. (18-20) are plotted on Fig. 3 in the form  $\frac{\tau}{P}$  as a function of  $I$ , together with the data of Fig. 13 from Ref. [3], kindly provided by the authors.

It appears that with adjusted values of  $I_0$  and  $\mu_2$ , Eqs. (19-20) are also compatible with the data. More elaborate comparisons should be carried out to see whether the aerial and submarine data can be usefully distinguished using the above equations.

For completeness, an interpolation between Eqs. (15) and (16) has been derived in the same manner and is available in the form of a short note [21].

#### IV. CONCLUSION

Considering a pair of grains rather than a single grain in a dense granular flow suggests that the typical stress

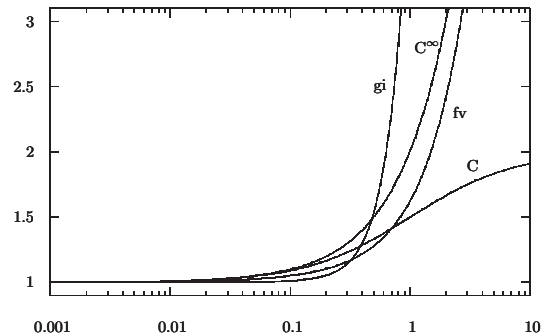


FIG. 2: Comparison of the present predictions with the empirical function  $\mu(I)$ . The curves labeled “gi” and “fv” are the plots of Eqs. (15-16) respectively. Curve “C” corresponds to Eq. (3), with  $\mu_c = 1$ ,  $\mu_2 = 2$  and  $I_0 = 1$ . Curve “ $C^\infty$ ” is obtained after removing the saturation, see Eq. (17).

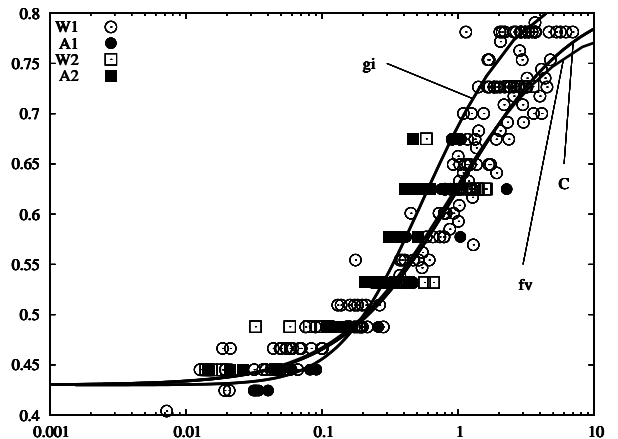


FIG. 3: Effective friction coefficient  $\mu(I)$ : data by Cassar *et al.* [3] kindly provided by the authors, and plot of three different functions. Open circles (W1): 112 $\mu\text{m}$  diameter beads in water. Filled circles (A1): same beads in air. Open squares (W2): 208 $\mu\text{m}$  beads in water. Filled squares (A2): same beads in air. Curve “C” corresponds to Eq. (3) with  $I_0 = 1$ ,  $\mu_c = 0.43$  and  $\mu_2 = 0.82$ . Curve “gi” represents Eq. (19) with  $I_0 = 0.2$ ,  $\mu_c = 0.43$  and  $\mu_2 = 0.7$ . Curve “fv” corresponds to Eq. (20) with  $I_0 = 0.7$ ,  $\mu_c = 0.43$  and  $\mu_2 = 1$ .

during the approach of two grains differs from that during their separation. This difference implies that the usual arguments used to derive an intrinsic timescale, whether when the grain inertia is dominant or when the fluid viscosity is dominant, now additionally predict the existence of a frictional threshold, with flow only when the ratio of the deviatoric stress to the pressure exceeds some finite value:  $\tau/P > \mu_c$ . However, the threshold value  $\mu_c$  (usually around 0.4) cannot be predicted by this approach.

Cassar *et al.* [3] had obtained a “universal” behaviour in the empirical form of Eq. (3), in terms of a dimen-

sionless parameter  $I$  with a different meaning in both regimes. The fact that two distinct laws are found for the inertial regime and for the viscous regime with the present approach indicates that the universal behaviour is perhaps only approximate. More involved investigations will be needed to test this universality.

## Acknowledgements

This work was supported by the Agence Nationale de la Recherche (ANR05).

- 
- [1] P. Coussot, *Rheometry of pastes, suspensions, and granular materials* (Wiley-Interscience, 2005).
  - [2] F. da Cruz, S. Emam, M. Prochnow, J.-N. Roux, and F. Chevoir, *Phys. Rev. E* **72**, 021309 (2005).
  - [3] C. Cassar, M. Nicolas, and O. Pouliquen, *Phys. Fluids* **17**, 103301 (2005).
  - [4] GDR MiDi, **14**, 341 (2004).
  - [5] P. Jop, Y. Forterre, and O. Pouliquen, *Nature* **441**, 727 (2006).
  - [6] Y. Forterre and O. Pouliquen, *Annu. Rev. Fluid Mech.* **40**, 1 (2008).
  - [7] P. G. Rognon, J.-N. Roux, M. Naaim, and F. Chevoir, *J. Fluid Mech.* **596** (2008).
  - [8] P. G. Rognon, J.-N. Roux, D. Wolf, M. Naaim, and F. Chevoir, *Europhys. Lett.* **74**, 644 (2006).
  - [9] P. Rognon, J. Roux, M. Naaim, and F. Chevoir, *Phys. Fluids* **19**, 058101 (2007).
  - [10] C. Campbell, *J. Fluid Mech.* **539**, 273 (2005).
  - [11] L. Silbert, G. Grest, R. Brewster, and A. Levine, *Phys. Rev. Lett.* **99**, 68002 (2007).
  - [12] R. Brewster, L. Silbert, G. Grest, and A. Levine, *Phys. Rev. E* **77**, 61302 (2008).
  - [13] F. da Cruz, F. Chevoir, D. Bonn, and P. Coussot, *Phys. Rev. E* **66**, 051305 (2002).
  - [14] P. Coussot, Q. Nguyen, H. Huynh, and D. Bonn, *J. Rheol.* **43**, 1 (2002).
  - [15] P. Coussot, H. Tabuteau, X. Chateau, L. Tocquer, and G. Ovarlez, *J. Rheol.* **50**, 975 (2006).
  - [16] P. G. Rognon, F. Chevoir, H. Bellot, F. Ousset, M. Naaim, and P. Coussot, *J. Rheol.* **52** (2008).
  - [17] N. Huang, G. Ovarlez, F. Bertrand, S. Rodts, P. Coussot, and D. Bonn, *Phys. Rev. Lett.* **94**, 28301 (2005).
  - [18] C. Barentin, E. Azanza, and B. Pouligny, *EPL (Europhysics Letters)* **66**, 139 (2004), URL <http://stacks.iop.org/0295-5075/66/139>.
  - [19] M. Lenoble, P. Snabre, and B. Pouligny, *Physics of Fluids* **17**, 073303 (pages 14) (2005), URL <http://link.aip.org/link/?PHF/17/073303/1>.
  - [20] P. Mills, P. Rognon, and F. Chevoir, **81**, 64005 (2008).
  - [21] P. Rognon and C. Gay, hal/axiv (2008), hal-00321845.